doi: 10.21608/esju.2025.330520.1047 *Research Article*

The Egyptian Statistical Journal (ESJ), 69 (1): 1-29

Homepage: https://esju.journals.ekb.eg/

The Egyptian Statistical Journal

Print ISSN 0542-1748– Online ISSN 2786-0086

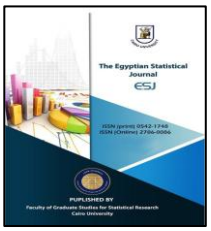

A New Bounded Distribution: Covid-19 Application

Yassmen Y. Abdelall [1] Gehad M. Ismail [2] Heba F. Nagy [1,*]

Received 24 October 24; revised 31 December 2024; accepted 14 January 2025

Keywords

Entropy measures; Estimation methods; Order statistics; Stress-strength; unit inverse power Lomax distribution.

Abstract

The modeling of proportional or percentage data through continuous distributions specified on the unit interval has become progressively relevant in various fields. This paper presents the unit inverse power Lomax distribution as a strong framework for such applications. The proposed model is thoroughly investigated, detailing its quantile function, moments, incomplete moments, probability-weighted moments, order statistics, stress-strength reliability function, and entropy measures. Ten distinct methods for estimation of the involved parameters, such as maximum likelihood, maximum product of spacings, minimum spacing absolute-log distance, least square, weighted least square, percentile, Anderson-Darling, left-tail Anderson-Darling estimation, left-tail Anderson-Darling second-order, and Cramer-von Mises, are studied. The significance of the presented model is demonstrated through comparative analysis with several existing statistical models via two applications using real datasets. This research underlines the potential advantages of the new distribution in accurately modeling proportional data, paving the way for further studies and practical applications.

1. Introduction

The Lomax distribution (LD), additionally recognized as the Pareto Type II distribution, is an important model for lifetime analysis and heavy-tailed phenomena, having a longer and heavier tail compared to the normal distribution. This particular instance of the generalized Pareto distribution was presented first by Lomax (1954). It is particularly useful in lifetime analysis as it can model phenomena where there is a high probability of observing large or extreme values, such as in the analysis of failure times or the distributions of income, Atkinson and Harrison (1978) used it to model failure rates of business. Holland et al. (2006) stated that the Lomax distribution can be used to model the distribution of computer file sizes on servers and in the biological sciences. The power Lomax (PL) distribution is a generalization of the LD that incorporates an extra shape parameter; that was presented by Rady et al. (2016).

✉ Corresponding author*: heba_nagy_84@cu.edu.eg

[1] Department of Mathematical Statistics, Faculty of Graduate Studies for Statistical Research, Cairo University, Giza, Egypt.

[2]Department of Basic Science, Higher Technological Institute, 10th of Ramadan, Egypt.

Inverted distributions offer unique properties and capabilities making them more applicable to certain lifetime phenomena. They are essential in different fields like financial literature, environmental studies, survival analysis, reliability theory, biological sciences, and life testing. Research has been dedicated to exploring inverted distributions and their uses in various domains. Now we mention some of these inverted distributions, for example, the inverse Weibull model proposed by Keller et al. (1982), inverted Lindley model by Sharma et al. (2015), inverted Kumaraswamy model by Abd AL-Fattah et al. (2017), inverted exponentiated Weibull model by Lee et al. (2017), inverted Nadarajah–Haghighi distribution by Tahir et al. (2018), inverted power Rama model by Onyekwere et al. (2020), inverse power Pranav model by Nwankwo et al. (2021), inverse Epsilon model by Jónás et al. (2022), inverse power Zeghdoudi model by Elgarhy et al. (2023), inverse continuous Bernoulli model by Opone and Chesneau (2024). The focus here is on the inverse power Lomax (IPL) model, which was introduced by Hassan and Nassr (2019). The key advantage of IPL model is its flexibility in modeling different types of functions. Specifically, the IPL distribution can accommodate decreasing and increasing-shaped hazard functions making it a versatile model for different real-world applications. This distribution is derived by applying a transformation to a random variable (rv) Z that is distributed as PL model. The transformation used is $Y = 1/Z$. The probability density function (PDF) and cumulative distribution function (CDF) of IPL model are defined respectively below:

$$g_{Y}(y;\psi,\varsigma,\nu) = \frac{\psi\varsigma}{\nu}\, y^{-(\varsigma+1)}\left(1+\frac{y^{-\varsigma}}{\nu}\right)^{-\psi-1}, \quad y,\psi,\varsigma,\nu>0, \tag{1}$$

$$G_{Y}(y;\psi,\varsigma,\nu) = \left(1+\frac{y^{-\varsigma}}{\nu}\right)^{-\psi}, \; y,\psi,\varsigma,\nu>0, \tag{2}$$

where ψ and ς are shape parameters and ν is scale parameter.

Statisticians focus on developing flexible probability distributions for datasets with a bound range (0,1), which are useful for modeling real-world phenomena such as ratios, rates, indices, proportions, and percentages. This area of research aims to minimize information loss and produce precise conclusions without introducing additional parameters. Here are a few of these recently released distributions: unit-Gompertz model proposed by Mazucheli et al. (2019), unit-inverse Gaussian model by Ghitany et al. (2019), unit modified Burr-III model by Haq et al. (2020), unit Teissier model by Krishna et al. (2022), unit inverse exponentiated Weibull model by Hassan and Alharbi (2023), unit Gumbel type-II model by Shafiq et al. (2023), unit upper truncated Weibull model by Okorie et al. (2023), unit generalized half-normal model by Mazucheli et al. (2023), unit exponential model by Bakouch et al. (2023) , unit two parameters Mirra model by Al-Omari et al. (2024).

Our research aims to provide a new unit flexible probability distribution called the unit inverse power Lomax (UIPL) distribution. It is based on the form of transformation $C = e^{-Y}$, where Y is IPL model has specific sub-models on the (0,1) interval. A comprehensive comparison of ten approaches to parameter estimation for the UIPL model was presented, along with an analysis of the performance of these estimators for distinct values of parameters and sample sizes.

Our research compared maximum likelihood (ML), maximum product of spacings (MPS), minimum spacing absolute-log distance (MSALD), least square (LS), weighted least square (WLS), percentile (Pe), Anderson-Darling (AD), left-tail Anderson-Darling (LAD), left-tail Anderson-Darling second order (LTS), and Cramer-von Mises (CM) estimation methods. Since it is challenging to investigate the features of various estimating techniques theoretically, the study conducted in-depth simulation studies to assess the relative absolute bias (RAbias) and mean squared error (MSE). The UIPL model was developed for several reasons, such as

- It is able to fit more accurately than other widely recognized unit interval distributions. To derive measures of uncertainty, moments, incomplete moments (IMs), probability-weighted moments (Pwm), and reliability.
- UIPL distribution parameters are evaluated using ten traditional estimating methods.
- Analyze the accuracy of various estimators using simulation studies.

The following sections of research are arranged as: composition of UIPL distribution is displayed in Section 2. Some of its key measures are computed in Section 3. Both the uncertainty measures and the stress-strength (S-S) reliability measure were covered in Section 4. In Section 5, ten distinct estimation methods are discussed. Section 6 discusses the simulation's results. Two real datasets are used in Section 7 to demonstrate the flexibility and applicability of the UIPL model. Finally, Section 8 affords the conclusion.

2. Unit Inverse Power Lomax Distribution

The UIPL model is suggested in this section. Let Y be a rv having IPL model, with parameters ψ, ς, ν and $C = e^{-Y}$, then the CDF of the bounded IPL distribution with support on (0, 1) is obtained as follows

$$F_C(c;\vartheta) = 1 - \left(1 + \frac{(-\ln c)^{-\varsigma}}{\nu}\right)^{-\psi} ; \quad 0 < c < 1, \psi, \varsigma, \nu > 0, \tag{3}$$

where $\vartheta = (\psi, \varsigma, \nu)$ is the vector of parameters, ψ and ς are shape parameters and ν is a scale parameter. The PDF of UIPL model is represented by

$$f_C(c,\vartheta) = \frac{\psi\varsigma}{\nu c}(-\ln c)^{-(\varsigma+1)}\left(1 + \frac{(-\ln c)^{-\varsigma}}{\nu}\right)^{-\psi-1} ; \quad 0 < c < 1, \ \psi, \varsigma, \nu > 0. \tag{4}$$

In addition, survival, and hazard rate functions (Hrf) of UIPL distribution, are given respectively as follows

$$S(c) = \left(1 + \frac{(-\ln c)^{-\varsigma}}{\nu}\right)^{-\psi}, \text{and } h(c) = \frac{\psi\varsigma}{\nu c}(-\ln c)^{-(\varsigma+1)}\left(1 + \frac{(-\ln c)^{-\varsigma}}{\nu}\right)^{-1}.$$

The cumulative Hrf, and Odds ratio are provided respectively as follows

$$H(c) = -\ln\left(\left(1+\frac{(-\ln c)^{-\varsigma}}{\nu}\right)^{-\psi}\right), \text{ and } O(c) = \frac{1-\left(1+\frac{(-\ln c)^{-\varsigma}}{\nu}\right)^{-\psi}}{\left(1+\frac{(-\ln c)^{-\varsigma}}{\nu}\right)^{-\psi}}.$$

Figure 1 displays the UIPL distribution PDF (4) forms using different parameter combinations. In accordance with the parameter values, the UIPL model's PDF is increasing, decreasing, and right skewed.

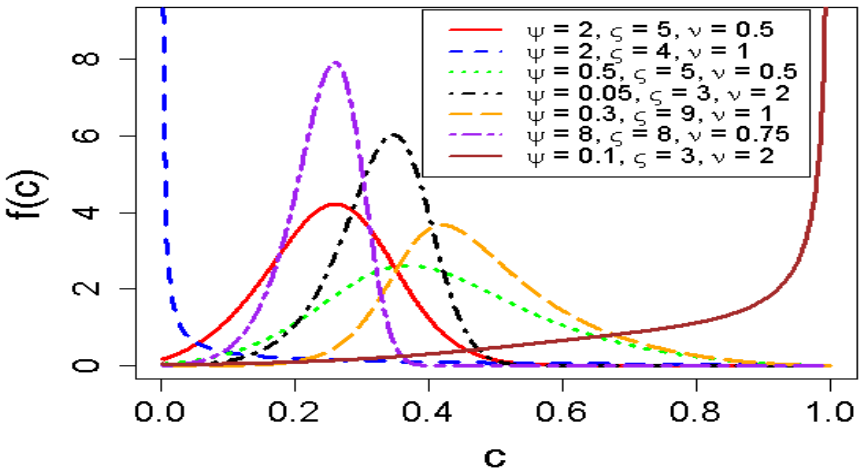

Figure 1: Distinct graphs of PDF for UIPL model

A graphical depiction for Hrf of the UIPL model using various parameter combinations is displayed in Figure 2. Hrf for UIPL model can be J-shaped, bathtub shaped, or increasing depending on the values for parameters.

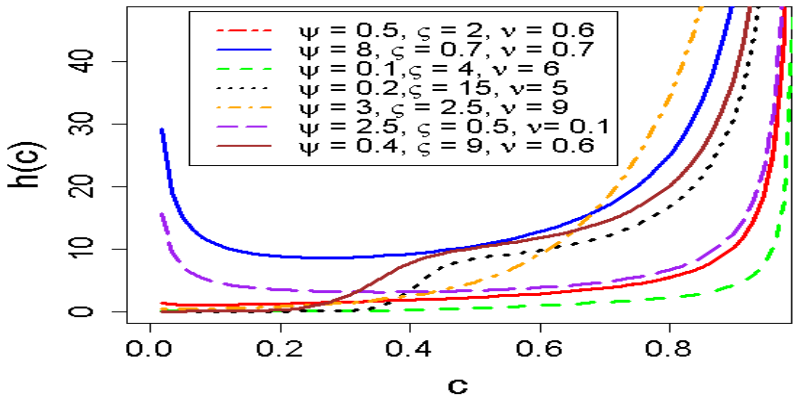

Figure 2: Distinct graphs of Hrf for UIPL model

3. Statistical Measures

In this section, some measures of the UIPL model are examined, especially quantile function, r^{th} moments, moment-generating function, incomplete moments, and probability-weighted moments.

3.1 Quantile Function

The quantile function of the UIPL model is given as $Q(m,\vartheta)=F^{-1}(m,\vartheta)$, where m is distributed as a Uniform $(0,1)$, it may be obtained by reversing the CDF in Equation (3) as follows

$$Q(m;\vartheta)=e^{-\left(\nu\left[(1-m)^{-\frac{1}{\psi}}-1\right]\right)^{-\frac{1}{\varsigma}}}, \quad 0<m<1. \tag{5}$$

The first, median, and third quantiles can be obtained by inserting $m=0.25$, 0.50 and, 0.75 respectively into (5).

3.2 Moments and Moment Generating Function

Moments are crucial statistical measures with diverse applications including characterizing probability distributions, enabling estimation and inference.

If C follows UIPL distribution with PDF defined in (4), then r^{th} moments of UIPL model

$$\mu'_r=\sum_{i=0}^{\infty}\frac{(-1)^i r^i \psi}{i!\,\nu^{i/\varsigma}}\,B\left(\frac{-i}{\varsigma}+1,\psi+\frac{i}{\varsigma}\right), \quad r=1,2,3,... \tag{6}$$

where r is a positive integer and $B(.,.)$ is incomplete beta function. The mean and variance of the UIPL model can be calculated from (6), respectively as follows

$$\mu'_1=\sum_{i=0}^{\infty}\frac{(-1)^i \psi}{i!\,\nu^{i/\varsigma}}\,B\left(\frac{-i}{\varsigma}+1,\psi+\frac{i}{\varsigma}\right),$$

and

$$\sigma^2=\sum_{i=0}^{\infty}\frac{(-1)^i 2^i \psi}{i!\,\nu^{i/\varsigma}}\,B\left(\frac{-i}{\varsigma}+1,\psi+\frac{i}{\varsigma}\right)-\left[\sum_{i=0}^{\infty}\frac{(-1)^i \psi}{i!\,\nu^{i/\varsigma}}\,B\left(\frac{-i}{\varsigma}+1,\psi+\frac{i}{\varsigma}\right)\right]^2.$$

Additionally, the generating function $\mu_C(t)$ for UIPL model is given as following

$$\mu_C(t)=E\left(e^{tC}\right)=\int_0^1 e^{tc}f(c)\,dc=\int_0^1\sum_{r=0}^{\infty}\frac{t^r}{r!}c^r f(c)\,dc=\sum_{r,i=0}^{\infty}\frac{(-1)^i r^i \psi t^r}{r!i!\,\nu^{i/\varsigma}}\,B\left(\frac{-i}{\varsigma}+1,\psi+\frac{i}{\varsigma}\right).$$

Table 1 presents numerical values for the first four moments: (μ'_1), (μ'_2), (μ'_3), (μ'_4), variance (σ^2), coefficient of skewness $(\Im_1)$, coefficient of kurtosis $(\Im_2)$, and coefficient of variation $(\Im_3)$ associated with selected parameter values for UIPL.

Table 1. Some numerical values for UIPL model

ν	ψ	ς	μ'_1	μ'_2	μ'_3	μ'_4	σ^2	$\Im_1$	$\Im_2$	$\Im_3$
0.7	3	7	0.2742	0.0798	0.0243	0.0077	0.0047	-0.3830	3.2592	0.2490
	5	9	0.2709	0.0760	0.0220	0.0065	0.0026	-0.6219	3.6472	0.1899
	7	12	0.2833	0.0818	0.0240	0.0071	0.0015	-0.7929	4.1270	0.1372
2	3	7	0.3270	0.1120	0.0398	0.0145	0.0051	-0.5189	3.5072	0.2183
	5	9	0.3122	0.1003	0.0330	0.0111	0.0029	-0.7088	3.8828	0.1710
	7	12	0.3147	0.1006	0.0326	0.0107	0.0016	-0.8437	4.3007	0.1266

Table 1 illustrates that when the values of ψ and ς increase, it is observed that the first four moments' measures decrease then increase, while the σ^2, $\Im_1$ and $\Im_3$ decrease. But $\Im_2$ increase. When the amount of ν rises, it is observed that in the first four moments, σ^2 and the $\Im_2$ increase while, $\Im_1$ and $\Im_3$ decrease. Based on the values of $\Im_1$ and $\Im_2$ in Table 1, the UIPL can be viewed to be left-skewed and leptokurtic.

The 3D plots of these measures for different values of ψ, ς and ν are displayed in Figure 3.

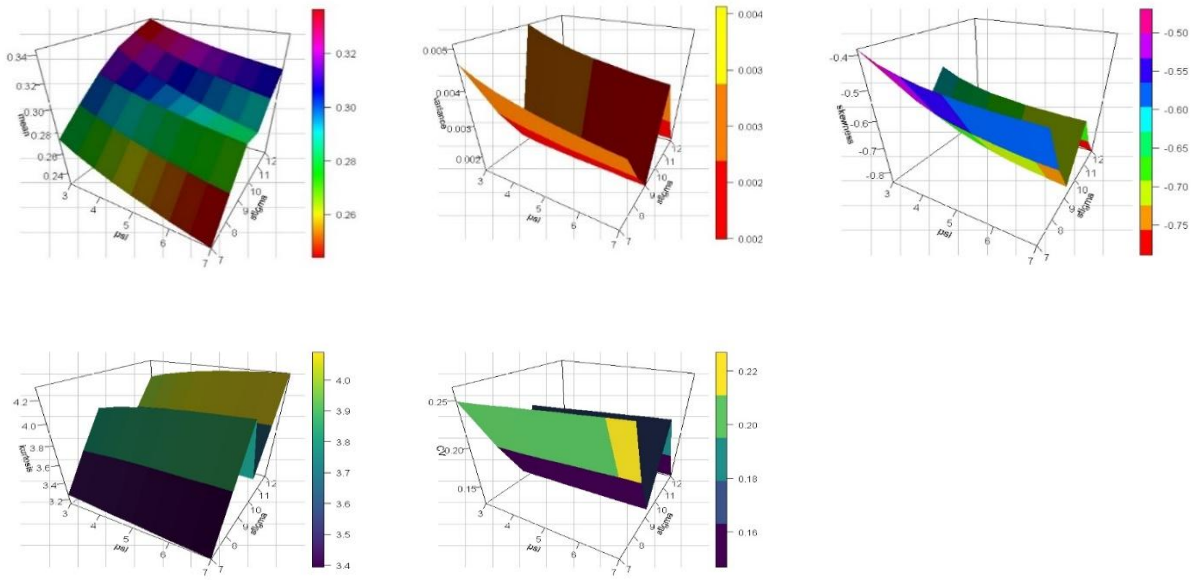

Figure 3: 3D plots of the key moment measures for UIPL, which are the mean, σ^2, $\Im_1$, $\Im_2$, and $\Im_3$, in that order from left to right.

This figure shows that the skewness varies approximately between -0.8 and -0.4 for the values of the parameters taken into consideration, suggesting a wide range of possibilities. As a result, the UIPL model can be negative-skewed and shows that the kurtosis varies approximately between 3 and 4.2 for the values of the parameters taken into consideration, which means that, the UIPL model can be leptokurtic.

The previously noted shape flexibility of the PDF and Hrf of the UIPLD is completed by these facts.

3.3 Incomplete Moment

A complete understanding of a distribution is essential for accurate modeling and analysis. The s^{th} incomplete moment of the UIPL is given as follows

$$\zeta_s(t) = \int_0^t c^s f(c;\psi,\varsigma,\nu)\, dc,$$

$$\zeta_s(t) = \sum_{i=0}^{\infty} \frac{(-1)^i (s)^i \psi}{i!(\nu)^{i/\varsigma-1}} B\left(\frac{-i}{\varsigma}, \psi + \frac{i}{\varsigma} + 1, \frac{(-\ln t)^{-\varsigma}}{\nu}\left(1 + \frac{(-\ln t)^{-\varsigma}}{\nu}\right)^{-1}\right), \tag{7}$$

where $B(.,.,.)$ is the upper incomplete beta function.

The first incomplete moment is obtained by inserting $s = 1$ in (7). The IMs are employed in various applications, including the calculation of Lorenz curve. This curve is widely used across different fields and disciplines. From (7), the Lorenz curve for a rv C is presented as

$$L_F(t) = \frac{1}{E(C)} \int_0^t c\, f(c;\psi,\varsigma,\nu)\, dc = \frac{1}{E(C)} \sum_{i=0}^{\infty} \frac{(-1)^i \psi}{i!(\nu)^{i/\varsigma-1}} B\left(\frac{-i}{\varsigma}, \psi + \frac{i}{\varsigma} + 1, \frac{(-\ln t)^{-\varsigma}}{\nu}\left(1 + \frac{(-\ln t)^{-\varsigma}}{\nu}\right)^{-1}\right).$$

3.4 Probability Weighted Moments

Greenwood et al. (1979) introduced the Pwm as an expectation of multiplication of two certain functions of a rv C given two positive integers, r and k. The Pwm is obtained by

$$\square_{r,k} = E\left(C^r F(c)^k\right) = \int_0^1 \left(c^r (F(c))^k f(c)\right) dc,$$

$$\square_{r,k} = \sum_{i=0}^{\infty} \frac{(-1)^i r^i \psi}{(\nu)^{i/\varsigma} i!} \sum_{j=0}^{k} (-1)^j \binom{k}{j} B\left(\frac{-i}{\varsigma} + 1, \psi(j+1) + \frac{i}{\varsigma}\right).$$

3.5 Order Statistics

Order statistics play a vital role in probability and statistical inference, especially in reliability and lifetime data analysis. In this subsection the p^{th} order statistics and the ℓ^{th} moment of order statistics are presented.

Let $c_{p:n}; p = 1,...,n$ be an n ordered random sample from UIPL with CDF in (3) and PDF in (4).

Then, according to Mood et al. (1950) the PDF of p^{th} order statistics is provided by

$$g_{p:n}(c) = \frac{n!}{(p-1)!(n-p)!}\left(F_C(c)\right)^{p-1}\left(1 - F_C(c)\right)^{n-p} f_C(c), \quad 0 < c < 1. \tag{8}$$

By inserting (3) and (4) into (8), the PDF of p^{th} order statistics for the UIPL is given as follows

$$g_{p:n}(c)=\frac{n!}{(p-1)!(n-p)!}\frac{\psi\varsigma}{\nu c}(-\ln c)^{-(\varsigma+1)}\left(1-\left(1+\frac{(-\ln c)^{-\varsigma}}{\nu}\right)^{-\psi}\right)^{p-1} \times\left(1+\frac{(-\ln c)^{-\varsigma}}{\nu}\right)^{-\psi(n-p+1)-1}. \quad (9)$$

The smallest and largest order statistics are obtained by inserting $p=1$ and $p=n$ respectively into (9),as follows

The PDF of the smallest order statistics is obtained as

$$g_{1:n}(c)=n[1-F(c)]^{n-1}[f(c)]=n\frac{\psi\varsigma}{\nu c}(-\ln c)^{-(\varsigma+1)}\left(1+\frac{(-\ln c)^{-\varsigma}}{\nu}\right)^{-\psi n-1}.$$

The PDF of the largest order statistics is obtained as

$$g_{n:n}(c)=n\left[F(c)\right]^{n-1}\left[f(c)\right]=n\left[1-\left(1+\frac{(-\ln c)^{-\varsigma}}{\nu}\right)^{-\psi}\right]^{n-1}\left[\frac{\psi\varsigma}{\nu c}(-\ln c)^{-(\varsigma+1)}\left(1+\frac{(-\ln c)^{-\varsigma}}{\nu}\right)^{-\psi-1}\right].$$

The ℓ^{th} moment of order statistics is obtained as

$$\mu^{\ell}_{p:n}=\int_0^1 c^{\ell} f_{(p:n)}(c)\,dc,$$

$$\mu^{\ell}_{p:n}=\frac{n!}{(p-1)!(n-p)!}\sum_{j=0}^{p-1}\binom{p-1}{j}(-1)^j\sum_{i=0}^{\infty}\frac{(-1)^i\ell^i\psi(\nu)^{-i/\varsigma}}{i!}B\left(1-\frac{1}{\varsigma},\psi(n-p+j+1)+\frac{1}{\varsigma}\right).$$

4. Uncertainty Measures and Stress-Strength Reliability

In this section, the most well-known measures of uncertainty in relation to UIPL model were explored. Specifically, Rényi entropy, exponential entropy, Tsallis entropy, Arimoto entropy, Havarda and Charvát entropy, extropy, weighted extropy, and cumulative residual extropy. Also, the stress- strength reliability of UIPL model is discussed.

4.1 Uncertainty Measures

There are various ways to measure the entropy of the UIPL model. A thorough grasp of the uncertainty and complexity of this distribution can be obtained by looking at various uncertainty measures.

a) Rényi entropy

According to Rényi (1961) the Rényi entropy is denoted as (R_{δ}) of a rv C is mathematically specified by

$$R_{\delta} = (1-\delta)^{-1} \log\left(\int_0^1 (f(c))^{\delta} dc \right), \ \delta > 0 \text{ and } \delta \neq 1, \tag{10}$$

where δ is the entropy order. The (R_{δ}) of the UIPL is obtained by using PDF in (4) into (10) as follows

$$R_{\delta} = (1-\delta)^{-1} \log\left(\frac{\psi^{\delta} \varsigma^{\delta}}{\nu^{\delta}} \int_0^1 c^{-\delta} (-\ln c)^{-\delta(\varsigma+1)} \left(1 + \frac{(-\ln c)^{-\varsigma}}{\nu}\right)^{-\delta(\psi+1)} dc \right)$$

$$= (1-\delta)^{-1} \log\left(\sum_{i=0}^{\infty} \frac{\psi^{\delta} \varsigma^{\delta-1} (\delta-1)^{i} \nu^{\frac{1}{\varsigma}(\delta-i-1)}}{i!} B\left(\delta + \frac{1}{\varsigma}(\delta-i-1), \delta\psi + \frac{1}{\varsigma}(i-\delta+1)\right) \right).$$

b) Exponential Entropy

The Exponential entropy proposed by Campbell (1966) denoted as (E_{δ}) of a rv C is expressed mathematically by

$$E_{\delta} = \left(\int_0^1 (f(c))^{\delta} dc \right)^{\frac{1}{1-\delta}}, \delta > 0 \text{ and } \delta \neq 1,$$

$$= \left(\sum_{i=0}^{\infty} \frac{\psi^{\delta} \varsigma^{\delta-1} (\delta-1)^{i} \nu^{\frac{1}{\varsigma}(\delta-i-1)}}{i!} B\left(\delta + \frac{1}{\varsigma}(\delta-i-1), \delta\psi + \frac{1}{\varsigma}(i-\delta+1)\right) \right)^{\frac{1}{1-\delta}}.$$

c) **Tsallis Entropy**

The Tsallis entropy which was presented by Tsallis (1988) denoted as (T_{δ}) of a rv C is expressed mathematically by

$$T_{\delta} = (\delta-1)^{-1} \left[1 - \left(\int_0^1 f(c)^{\delta} dc \right) \right], \delta \in R, \delta \neq 1, \delta > 0,$$

$$= (\delta-1)^{-1} \left[1 - \left(\sum_{i=0}^{\infty} \frac{\psi^{\delta} \varsigma^{\delta-1} (\delta-1)^{i} \nu^{\frac{1}{\varsigma}(\delta-i-1)}}{i!} B\left(\delta + \frac{1}{\varsigma}(\delta-i-1), \delta\psi + \frac{1}{\varsigma}(i-\delta+1)\right) \right) \right].$$

d) Arimoto Entropy

Arimoto (1971) presented the Arimoto entropy, which was denoted by (A_{δ}) of a rv C is acquired by

$$A_{\delta}=\frac{\delta}{1-\delta}\left[\left(\int_0^1 (f(c))^{\delta}\, dc\right)^{\frac{1}{\delta}}-1\right],\ \delta\neq 1,\delta>0,$$

$$=\frac{\delta}{1-\delta}\left[\left(\sum_{i=0}^{\infty}\frac{\psi^{\delta}\varsigma^{\delta-1}(\delta-1)^{i}\nu^{\frac{1}{\varsigma}(\delta-i-1)}}{i!}B\left(\delta+\frac{1}{\varsigma}(\delta-i-1),\delta\psi+\frac{1}{\varsigma}(i-\delta+1)\right)\right)^{\frac{1}{\delta}}-1\right].$$

e) Havarda and Charvát Entropy

The Havarda and Charvát entropy proposed by Havrda and Charvát (1967) is denoted as (HC_{δ}) of a rv C is defined mathematically by

$$HC_{\delta}=\frac{1}{2^{1-\delta}-1}\left[\left(\int_0^1 (f(c))^{\delta}\, dc\right)^{\frac{1}{\delta}}-1\right],\delta\neq 1,\ \delta>0,$$

$$=\frac{1}{2^{1-\delta}-1}\left[\left(\sum_{i=0}^{\infty}\frac{\psi^{\delta}\varsigma^{\delta-1}(\delta-1)^{i}\nu^{\frac{1}{\varsigma}(\delta-i-1)}}{i!}B\left(\delta+\frac{1}{\varsigma}(\delta-i-1),\delta\psi+\frac{1}{\varsigma}(i-\delta+1)\right)\right)^{\frac{1}{\delta}}-1\right].$$

Table 2 displays various numerical values for certain measures of entropy for UIPL model using a set of predetermined parameter values are presented.

Table 2. UIPL entropy measures

δ	ν	ς	ψ	R_{δ}	E_{δ}	T_{δ}	A_{δ}	HC_{δ}
0.2	0.5	3	1.5	-0.2751	0.8386	-0.2469	-0.1668	-0.2666
		3.5	2	-0.4274	0.7607	-0.3620	-0.2048	-0.3907
		4	2.5	-0.5578	0.6998	-0.4500	-0.2232	-0.4857
		4.5	4.5	-0.8220	0.5909	-0.6024	-0.2407	-0.6503
		5	5.5	-0.9136	0.5573	-0.6481	-0.2435	-0.6996
		5.5	6.5	-0.9837	0.5328	-0.6809	-0.2451	-0.7351
0.7		3	1.5	-0.5241	0.9539	-0.4850	-0.4694	-0.6295
		3.5	2	-0.6972	0.9392	-0.6291	-0.6027	-0.8165
		4	2.5	-0.8292	0.9281	-0.7341	-0.6978	-0.9527
		4.5	4.5	-1.0714	0.9081	-0.9163	-0.8591	-1.1892
		5	5.5	-1.1574	0.9011	-0.9778	-0.9124	-1.2691
		5.5	6.5	-1.2301	0.8952	-1.0287	-0.9561	-1.3351
1.2		3	1.5	-0.6289	0.9752	-0.6702	-0.6630	-1.0354
		3.5	2	-0.7852	0.9691	-0.8502	-0.8389	-1.3136

δ	ν	ς	ψ	R_δ	E_δ	T_δ	A_δ	HC_δ
		4	2.5	-0.9225	0.9638	-1.0131	-0.9972	-1.5652
		4.5	4.5	-1.1601	0.9547	-1.3058	-1.2799	-2.0174
		5	5.5	-1.2528	0.9511	-1.4238	-1.3932	-2.1997
		5.5	6.5	-1.3339	0.9480	-1.5288	-1.4938	-2.3619

Table 2 indicates that when the value of δ increase while the value of $\psi, \varsigma, \upsilon,$ stay constant the values of R_δ, T_δ, A_δ and HC_δ decrease implying less information needed, but the value of E_δ increase which implies that more information is needed to accurately predict the distribution (high uncertainty). When the values of ψ and ς increase, the values of these different entropies decrease, implying that there is less variability. For the values of the parameters taken into consideration, the lowest entropy values were obtained when the entropy order value was equal to 1.2, except for E_δ. The degree of uncertainty or variability in a random variable is measured by entropy. The more uncertain the data, the higher the entropy value. There are many applications for these different entropies, especially in physics by Beck (2009) , stock exchanges by Jiang et al. (2008), income distribution by Soares et al. (2016) , and earthquakes by Abe and Suzuki (2003).

f) Extropy

A measure of uncertainty named extropy was presented by Lad et al. (2015). Statistically, the extropy may be used to assess the accuracy of predicting distributions using the total log scoring method, in commercial or scientific areas such as astronomical measurements of heat distributions in galaxies. The extropy denoted as (τ) for UIPL is acquired by

$$\tau = \frac{-1}{2}\int_0^1 f(c;\vartheta)^2\, dc = \frac{-1}{2}\left[\sum_{i=0}^{\infty} \frac{\psi^2 \varsigma \nu^{\frac{1}{\varsigma}(1-i)}}{i!} B\left(\frac{1}{\varsigma}(1-i)+2, 2\psi+\frac{1}{\varsigma}(i-1)\right)\right].$$

Extropy is a different measure of uncertainty and has some advantages. One major advantage of extropy is its ease of computation, making it highly valuable for exploring potential applications, such as inferential methods (see Mohammadi et al. 2024). One of the reasons for depending on cumulative residual extropy, distribution functions, such as power-Pareto, generalized lambda, and Govindarajulu distributions, exist even in the absence of probability density functions, (see Husseiny et al. (2024). In contrast, the survival function is the basis for the cumulative residual extropy measure.

There are several types to measure the extropy for the UIPL model, particularly weighted and cumulative residual extropies.

g) Weighted Extropy

The weighted extropy is denoted as (τ^w) is another analogue of the weighted entropy that was suggested by Balakrishnan et al. (2022). It can be clarified as

$$\tau^w = \frac{-1}{2}\int_0^1 c\, f(c;\vartheta)^2\, dc = \frac{-1}{2}\left[\psi^2 \varsigma \nu^{\frac{1}{\varsigma}} B\left(\frac{1}{\varsigma}+2\,,\, 2\psi-\frac{1}{\varsigma}\right)\right].$$

h) Cumulative Residual Extropy

The cumulative residual extropy is denoted as (Ω), which was proposed by Jahanshahi et al. (2020) is obtained as

$$\Omega = \frac{-1}{2}\int_0^1 \bar{F}(c;\vartheta)^2\, dc = \frac{-1}{2}\left[\sum_{i=0}^{\infty}\frac{(-1)^i}{\varsigma(\nu)^{1/\varsigma(i+1)}\, i!}B\left(\frac{-1}{\varsigma}(i+1), \frac{1}{\varsigma}(i+1)+2\psi\right)\right].$$

Table 3 introduces some specific numerical values for extropy, weighted extropy and cumulative residual extropy measures for UIPL model using a set of predetermined parameter values.

Table 3. UIPL extropy measures

ν	ς	ψ	τ	τ^w	Ω
0.5	3	1.5	-1.5783	-0.1999	-0.0764
	3.5	2	-1.2641	-0.2348	-0.0739
	4	2.5	-1.3690	-0.2743	-0.0751
	4.5	4.5	-1.7282	-0.3017	-0.0651
	5	5.5	-1.9101	-0.3440	-0.0683
	5.5	6.5	-2.0856	-0.3884	-0.0719
0.9	3	1.5	-1.0515	-0.2432	-0.1025
	3.5	2	-1.0887	-0.2777	-0.0966
	4	2.5	-1.2525	-0.3178	-0.0954
	4.5	4.5	-1.5754	-0.3438	-0.0823
	5	5.5	-1.7663	-0.3869	-0.0842
	5.5	6.5	-1.9498	-0.4322	-0.0868

Table 3 indicates that when the values of ψ and ς raise, the values of the τ^w decrease indicating low likelihood of rare events and values of τ and Ω increase representing higher likelihood of rare events. When the values of ν increases, the values of the τ^w and Ω decrease and values of τ increase.

4.3. Stress-Strength Reliability

According to Birnbaum (1956), The notation S-S reliability is denoted by $\Re = p\left[C_2 < C_1\right]$, where C_1 represents the component strength having UIPL (ψ_1, ς, ν) and C_2 represents the component stress having UIPL (ψ_2, ς, ν). Then $\Re$ is acquired by

$$\Re = \int_0^1 \frac{\psi_1 \varsigma}{\nu c}(-\ln c)^{-(\varsigma+1)}\left(1+\frac{(-\ln c)^{-\varsigma}}{\nu}\right)^{-\psi_1-1}\left\{1-\left(1+\frac{(-\ln c)^{-\varsigma}}{\nu}\right)^{-\psi_2}\right\} dc,$$

$$\Re = \frac{\psi_2}{\psi_1+\psi_2}.$$

5. Parameter Estimation

Ten different strategies for estimating the vector of parameters $\vartheta=(\psi,\varsigma,\nu)$, ML, MPS, MSALD, LS, WLS, Pe, AD, LAD, LTS and CM, associated with the UIPL distribution with PDF given by (4) are discussed in this section, For additional details regarding the estimation techniques employed, see Aguilar et al. (2019) and Ali et al. (2020).

5.1 Maximum Likelihood

Let $c_1,c_2,...,c_n$ be a random sample of size n from a rv C with UIPL model. The log-likelihood function for estimating the vector of parameters ϑ is pointed by ℓ is

$$\ell = n\ln(\psi)+n\ln(\varsigma)-n\ln(\nu)-\sum_{i=1}^{n}\ln(c_i)-(\varsigma+1)\sum_{i=1}^{n}\ln(-\ln c_i)-(\psi+1)\sum_{i=1}^{n}\ln\left(1+\frac{1}{\nu}(-\ln c_i)^{-\varsigma}\right). \tag{11}$$

The desired ML estimators are acquired by maximizing the log-likelihood function. Differentiating (11) with respect to each parameter ψ,ς and ν respectively, results in following equations

$$\frac{\partial\ell}{\partial\psi}=\frac{n}{\psi}-\sum_{i=1}^{n}\ln\left(1+\frac{1}{\nu}(-\ln c_i)^{-\varsigma}\right), \tag{12}$$

$$\frac{\partial\ell}{\partial\varsigma}=\frac{n}{\varsigma}-\sum_{i=1}^{n}\ln(-\ln c_i)+(\psi+1)\sum_{i=1}^{n}\frac{(-\ln c_i)^{-\varsigma}\ln(-\ln c_i)}{\left(\nu+(-\ln c_i)^{-\varsigma}\right)}, \tag{13}$$

and

$$\frac{\partial\ell}{\partial\nu}=\frac{-n}{\nu}+(\psi+1)\sum_{i=1}^{n}\frac{(-\ln c_i)^{-\varsigma}}{\nu^2+\nu(-\ln c_i)^{-\varsigma}}. \tag{14}$$

The ML estimators of ϑ, say $\hat{\vartheta}=(\hat{\psi},\hat{\varsigma},\hat{\nu})$ are acquired by Equating (12), (13) and (14) by zero and solving them numerically using R programming language.

5.2 Maximum Product Spacings

An alternative estimation technique to ML is the MPS method. Cheng and Amin (1979) presented this method, the MPS maximizes the product of the spacings between ordered data points. It is especially helpful for estimating parameters of continuous probability distributions.
Let $c_{1:n},...,c_{n:n}$ be an ordered random sample of size n from UIPL model, the MPS estimators, $\hat{\vartheta}=(\hat{\psi},\hat{\varsigma},\hat{\nu})$ are given by maximizing the following function

$$\Phi(\vartheta)=\frac{1}{n+1}\sum_{i=1}^{n+1}\log(\zeta_{i,n}(\vartheta)),$$

where $\zeta_{i,n}(\vartheta)=F(c_{i:n})-F(c_{i-1:n}),F(c_{0:n})=0$ and $F(c_{n+1:n})=1$.

$$\zeta_{i,n}(\vartheta)=\left(1-\left(1+\frac{(-\ln c_{i:n})^{-\varsigma}}{\nu}\right)^{-\psi}\right)-\left(1-\left(1+\frac{(-\ln c_{i-1:n})^{-\varsigma}}{\nu}\right)^{-\psi}\right). \tag{15}$$

5.3 Minimum Spacing Absolute -Log Distance

The MSALD estimators, $\hat{\vartheta}=(\hat{\psi},\hat{\varsigma},\hat{\nu})$ are acquired by minimizing the following equation

$$\varepsilon(\vartheta)=\sum_{i=1}^{n+1}\left|\log\zeta_{i,n}(\vartheta)-\log\left(\frac{1}{n+1}\right)\right|,$$

where $\zeta_{i,n}(\vartheta)$ is given in (15).

5.4 Least Square

A mathematical model's parameters are estimated by minimizing the sum of the squares of the variations between the values that are observed and those that are predicted. The LS estimators, $\hat{\vartheta}=(\hat{\psi},\hat{\varsigma},\hat{\nu})$ are acquired by minimizing the following equation

$$\iota(\vartheta)=\sum_{i=1}^{n}\left[F(c_{i:n})-\frac{i}{n+1}\right]^2=\sum_{i=1}^{n}\left[\left(1-\left(1+\frac{(-\ln c_{i:n})^{-\varsigma}}{\nu}\right)^{-\psi}\right)-\frac{i}{n+1}\right]^2.$$

5.5 Weighted Least Squares

This statistical technique involves giving each observation a different weight in order to estimate the parameters of a probability model. The WLS estimators, $\hat{\vartheta}=(\hat{\psi},\hat{\varsigma},\hat{\nu})$ are calculated to minimize the following equation

$$W(\vartheta)=\sum_{i=1}^{n}\frac{(n+1)^2(n+2)}{i(n-i+1)}\left[F(c_{i:n})-\frac{i}{n+1}\right]^2=\sum_{i=1}^{n}\frac{(n+1)^2(n+2)}{i(n-i+1)}\left[\left(1-\left(1+\frac{(-\ln c_{i:n})^{-\varsigma}}{\nu}\right)^{-\psi}\right)-\frac{i}{n+1}\right]^2.$$

5.6 Percentile Estimation

The Pe estimators, $\hat{\vartheta}=(\hat{\psi},\hat{\varsigma},\hat{\nu})$ are acquired by minimizing the following function

$$P(\vartheta)=\sum_{i=1}^{n}\left[\ln(\frac{i}{n+1})-\ln\left(F(c_{i:n},\vartheta)\right)\right]^2,$$

$$P(\vartheta)=\sum_{i=1}^{n}\left[\ln(\frac{i}{n+1})-\ln\left(1-\left(1+\frac{(-\ln c_{i:n})^{-\varsigma}}{\nu}\right)^{-\psi}\right)\right]^2,$$

where $\frac{i}{n+1}$ is an unbiased estimator of $F(c_{i:n},\vartheta)$.

5.7 Anderson-Darling Estimation

The AD estimators, $\hat{\vartheta}=(\hat{\psi},\hat{\varsigma},\hat{\nu})$ are acquired by minimizing the following equation

$$A_n(\vartheta)=-n-\sum_{i=1}^{n}\frac{(2i-1)}{n}\left\{\log\left[F(c_{i:n};\vartheta)\right]+\log\left[S(c_{n+1-i:n};\vartheta)\right]\right\},$$

$$A_n(\vartheta) = -n - \sum_{i=1}^{n} \frac{(2i-1)}{n} \left\{ \log\left[1 - \left(1 + \frac{(-\ln c_{i:n})^{-\varsigma}}{\nu} \right)^{-\psi} \right] + \log\left[\left(1 + \frac{(-\ln c_{n+1-i:n})^{-\varsigma}}{\nu} \right)^{-\psi} \right] \right\}.$$

5.8 Left – Tail Anderson-Darling Estimation

The LAD estimation method focuses on estimating the parameters of a distribution, with a particular emphasis on the left tail. These methods utilize the Anderson-Darling statistic, which quantifies how well a distribution fits the observed data. Estimation process involves minimizing the CDF of the UIPL model for the ordered rvs to determine the model parameters.

The LAD estimators, $\hat{\vartheta} = (\hat{\psi}, \hat{\varsigma}, \hat{\nu})$ are acquired by minimizing the following function

$$L(\vartheta) = -\frac{3}{2} n \sum_{i=1}^{n} F(c_{i:n}; \vartheta) - \frac{1}{n} \sum_{i=1}^{n} (2i-1) \log\left[F(c_{i:n}; \vartheta) \right] + \log\left[F(c_{i:n}; \vartheta) \right],$$

$$L(\vartheta) = -\frac{3}{2} n \sum_{i=1}^{n} \left(1 - \left(1 + \frac{(-\ln c_{i:n})^{-\varsigma}}{\nu} \right)^{-\psi} \right)$$

$$- \frac{1}{n} \sum_{i=1}^{n} (2i-1) \log\left[1 - \left(1 + \frac{(-\ln c_{i:n})^{-\varsigma}}{\nu} \right)^{-\psi} \right] + \log\left[1 - \left(1 + \frac{(-\ln c_{i:n})^{-\varsigma}}{\nu} \right)^{-\psi} \right].$$

5.9 Left–Tail Anderson-Darling Estimation Second Order

The LTS estimators, $\hat{\vartheta} = (\hat{\psi}, \hat{\varsigma}, \hat{\nu})$ are acquired by minimizing the function

$$Le(\vartheta) = 2 \sum_{i=1}^{n} \log\left[F(c_{i:n}; \vartheta) \right] + \frac{1}{n} \sum_{i=1}^{n} \frac{(2i-1)}{F(c_{i:n}; \vartheta)},$$

$$Le(\vartheta) = 2 \sum_{i=1}^{n} \log\left[1 - \left(1 + \frac{(-\ln c_{i:n})^{-\varsigma}}{\nu} \right)^{-\psi} \right] + n^{-1} \sum_{i=1}^{n} (2i-1) \left(1 - \left(1 + \frac{(-\ln c_{i:n})^{-\varsigma}}{\nu} \right)^{-\psi} \right)^{-1}.$$

5.10 Cramer- Von Mises Estimation

The CM estimators, $\hat{\vartheta} = (\hat{\psi}, \hat{\varsigma}, \hat{\nu})$ are acquired by minimizing the following function

$$Cm(\vartheta) = \frac{1}{12n} + \sum_{i=1}^{n} \left[F(c_{i:n}; \vartheta) - \frac{2i-1}{2n} \right]^2 = \frac{1}{12n} + \sum_{i=1}^{n} \left[\left(1 - \left(1 + \frac{(-\ln c_{i:n})^{-\varsigma}}{\nu} \right)^{-\psi} \right) - \frac{2i-1}{2n} \right]^2.$$

6. Numerical Simulation

This section focuses on simulation work, which is considered one of the most critical parts of the research. The performance of distinct estimation techniques proposed for estimating the parameters of UPL model is investigated by analyzing detailed simulation results. Different sample sizes $n = 50, 80, 150\,(100)\,350$, and various parameter values, Set 1: $\vartheta = (0.6, 2.5, 0.2)$,

Set 2: $\vartheta = (0.6, 2.8, 0.2)$, Set 3: $\vartheta = (0.4, 2.5, 0.07)$ are used. Additionally, 1000 random samples are generated from the UIPL model based on (5). Finally, RAbias and MSE were calculated using the following equations as

$$RAbias_{(\hat{\vartheta})} = \frac{1}{1000}\sum_{\kappa=1}^{1000}\left|\frac{\hat{\vartheta}_{\kappa} - \vartheta_{\kappa}}{\vartheta_{\kappa}}\right|,\ MSE_{(\hat{\vartheta})} = \frac{1}{1000}\sum_{\kappa=1}^{1000}(\hat{\vartheta}_{\kappa} - \vartheta_{\kappa})^2$$

Simulation algorithm

1. Indicate the population parameter values.
2. Using the inverse CDF in (5), a random sample of size $n = 50, 80, 150\ (100)\ 350$ is generated.
3. Apply estimation techniques to assess the estimates' values.
4. Utilize the various estimation techniques to determine the RAbias and MSE for each parameter.
5. The simulation results are presented in Tables 4–6. The following are displayed as below
    1. Based on various estimation techniques, the RAbias of all estimates decrease as *n* increase (see Tables 4–6).
    2. The AD of ς for all sets has the smallest RAbias value for all different sample sizes (see Tables 4–6).
    3. The lowest MSE obtained for the ς estimate was in set 1 compared to the rest of the sets (see Tables 4 and 6).
    4. The MSEs for the ς estimate increase as value of ς increases (see Tables 4 and 5).
    5. The lowest MSE obtained for the ψ estimate was in set 1 compared to the rest of the sets (see Tables 4 and 6).
    6. From set 1 and set 3 it can be shown that , the MSEs for ψ and ν estimates decrease as values of ψ and ν decrease and ς estimate stay constant (see Tables 4 and 6).
    7. The MSEs for the ς estimate increase as value of ψ and ν decrease (see Tables 4 and 6)
    8. Tables 4 and 5 show that the AD of ν in set 1 and set 2 has the smallest MSE value for all different sample sizes.
    9. Table 6 shows that ML of ν in set 3 has the smallest MSE value for all different sample sizes.
    10. The MSEs of all estimates based on different techniques decrease for all chosen sets of parameters as the sample size increases (see Tables 4–6), and (see Figures 4–6), which display heatmaps of the MSEs of all estimates based on different techniques.
    11. In heatmaps the colors appear to range from dark to light, indicating a decrease in values of MSEs. Higher values are represented by darker hues, and lower values by lighter hues.
    12. Just looking at the heatmaps, we can see that the AD method is the lightest shade of color which indicates that it is less MSEs for all sets.
    13. Considering the outcomes of the simulation, the AD approach is typically the most effective estimation technique, whereas LTS is the least effective.

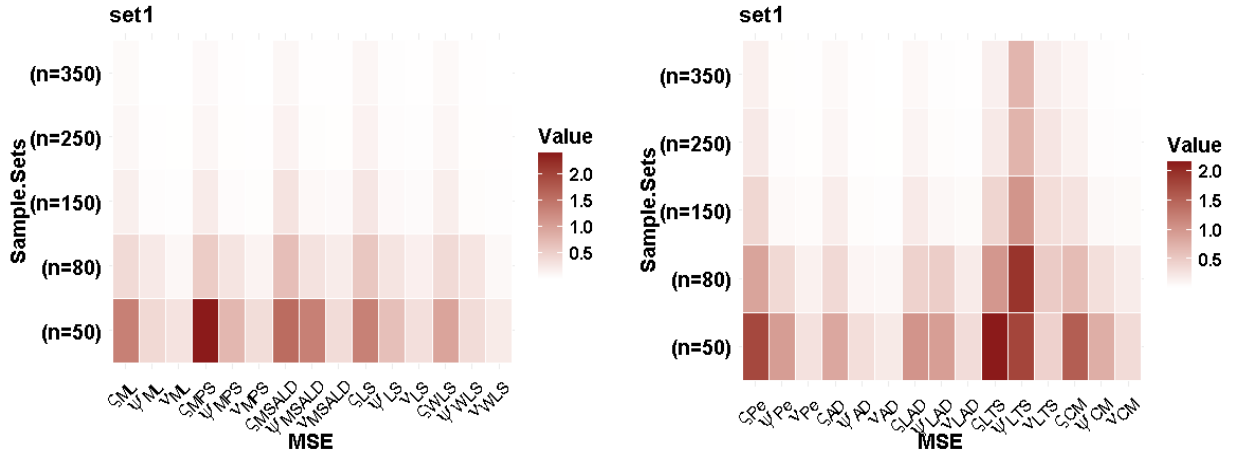

Figure 4: MSEs of all methods of set 1

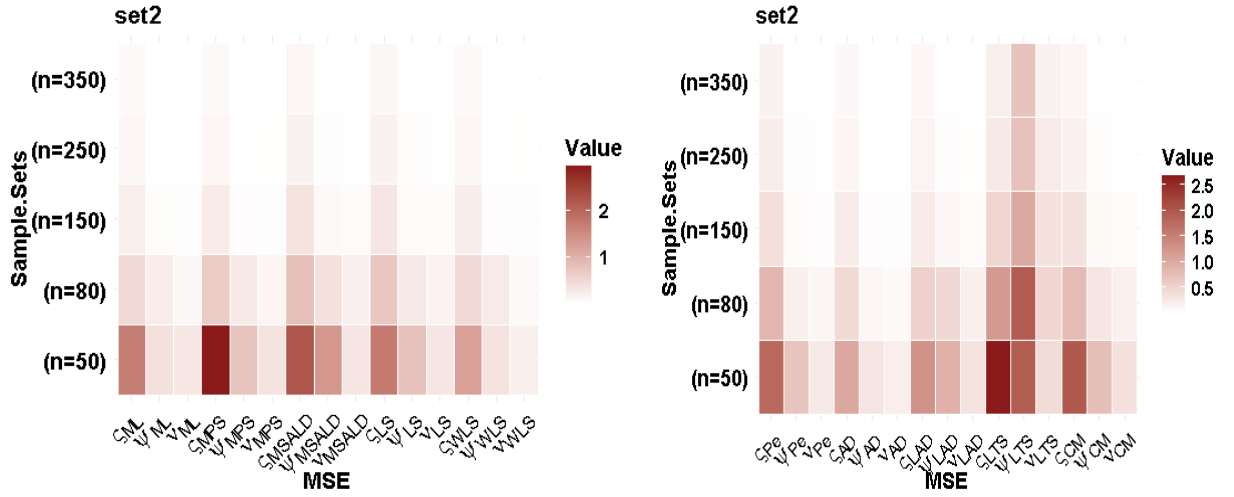

Figure 5: MSEs of all methods of set 2

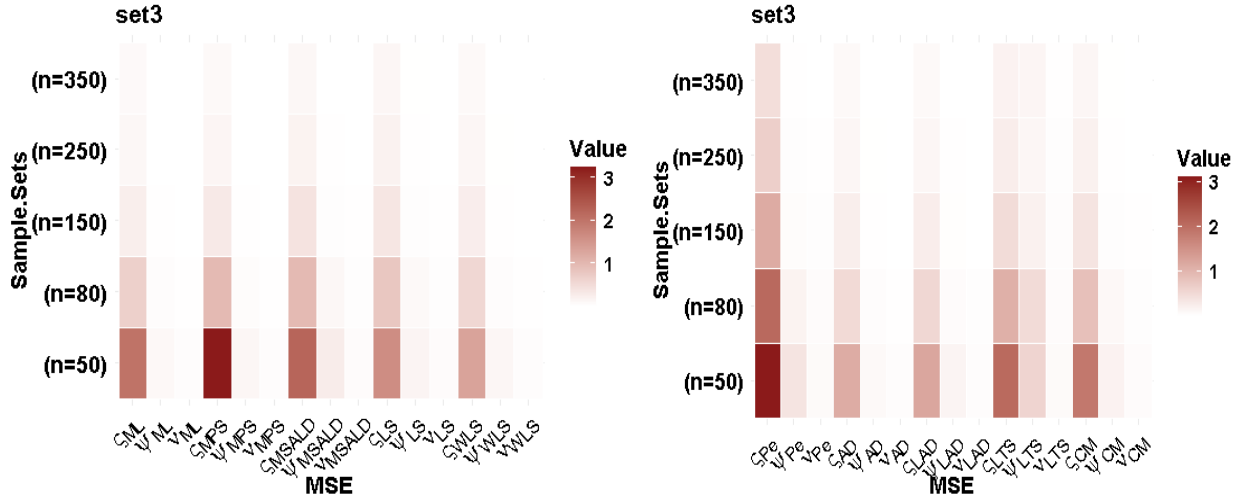

Figure 6: MSEs of all methods of set 3

Table 4. Parameter estimates of simulation results for Set 1

n			ML	MPS	MSALD	LS	WLS	Pe	AD	LAD	LTS	CM
50	RAbias	$\hat{\varsigma}$	0.1316	0.2272	0.1479	0.1117	0.0895	0.1632	0.0929	0.1054	0.1792	0.1471
		$\hat{\psi}$	0.2672	0.375	0.4833	0.3232	0.2295	0.2971	0.2226	0.4279	0.5236	0.3602
		$\hat{\nu}$	0.8095	0.9089	0.8727	0.8685	0.6846	0.7132	0.6819	0.9221	0.8321	0.8789
	MSE	$\hat{\varsigma}$	1.3553	2.3951	1.5782	1.3456	0.9613	1.7681	0.8352	1.0187	2.1531	1.5503
		$\hat{\psi}$	0.4053	0.7569	1.3545	0.6708	0.3677	0.9358	0.3176	0.9242	1.7917	0.7683
		$\hat{\nu}$	0.2953	0.3622	0.3702	0.3352	0.2173	0.2855	0.2064	0.3307	0.4344	0.3441
80	RAbias	$\hat{\varsigma}$	0.0525	0.0972	0.0669	0.0486	0.0375	0.0912	0.0418	0.0463	0.0849	0.0679
		$\hat{\psi}$	0.1587	0.1912	0.2292	0.2178	0.1623	0.1551	0.126	0.286	0.6443	0.2345
		$\hat{\nu}$	0.4385	0.5116	0.6836	0.6444	0.435	0.4996	0.4241	0.6862	1.0765	0.6658
	MSE	$\hat{\varsigma}$	0.3909	0.5411	0.6832	0.5909	0.3942	0.867	0.362	0.4282	0.9907	0.6392
		$\hat{\psi}$	0.2322	0.2839	0.3088	0.2826	0.2771	0.367	0.1011	0.4718	1.9503	0.3092
		$\hat{\nu}$	0.0927	0.1298	0.1994	0.1685	0.0853	0.1409	0.0813	0.192	0.4907	0.1816
150	RAbias	$\hat{\varsigma}$	0.0285	0.0516	0.0307	0.0246	0.0206	0.0521	0.0224	0.0251	0.0291	0.0342
		$\hat{\psi}$	0.0586	0.0735	0.1011	0.1011	0.0624	0.0537	0.0624	0.1142	0.4861	0.1066
		$\hat{\nu}$	0.1933	0.207	0.3363	0.3318	0.2131	0.2447	0.2095	0.3337	0.9604	0.3355
	MSE	$\hat{\varsigma}$	0.1757	0.2113	0.296	0.2612	0.1849	0.3843	0.1785	0.2032	0.4009	0.2721
		$\hat{\psi}$	0.04	0.046	0.0815	0.0761	0.042	0.0638	0.0398	0.0878	1.0163	0.0788
		$\hat{\nu}$	0.0293	0.0328	0.0654	0.0558	0.0294	0.0492	0.0289	0.0596	0.3266	0.0572
250	RAbias	$\hat{\varsigma}$	0.0139	0.0282	0.0146	0.0118	0.0089	0.0303	0.0107	0.0109	0.0038	0.0174
		$\hat{\psi}$	0.0367	0.0455	0.0527	0.0603	0.0412	0.0321	0.0402	0.0707	0.3917	0.063
		$\hat{\nu}$	0.1155	0.12	0.1765	0.1922	0.1332	0.1435	0.1287	0.2029	0.8084	0.1927
	MSE	$\hat{\varsigma}$	0.0899	0.1019	0.1394	0.1388	0.0976	0.2118	0.0963	0.1072	0.2102	0.1421
		$\hat{\psi}$	0.0204	0.0226	0.0318	0.0369	0.0226	0.0335	0.0216	0.04	0.7155	0.0375
		$\hat{\nu}$	0.0134	0.0146	0.0229	0.0247	0.0148	0.0231	0.0142	0.026	0.2475	0.025
350	RAbias	$\hat{\varsigma}$	0.0092	0.0194	0.0064	0.0045	0.0043	0.0223	0.0054	0.0047	0.0025	0.0085
		$\hat{\psi}$	0.0265	0.033	0.0445	0.0521	0.0346	0.024	0.0337	0.0556	0.339	0.0539
		$\hat{\nu}$	0.0867	0.0892	0.1469	0.1635	0.1118	0.1104	0.1083	0.16	0.6363	0.1636
	MSE	$\hat{\varsigma}$	0.0624	0.068	0.0956	0.097	0.0695	0.153	0.0676	0.0737	0.1548	0.0985
		$\hat{\psi}$	0.013	0.014	0.0213	0.0247	0.0156	0.023	0.015	0.0252	0.7002	0.025
		$\hat{\nu}$	0.0086	0.0092	0.015	0.0167	0.0104	0.0157	0.01	0.0162	0.1631	0.0168

Table 5. Parameter estimates of simulation results for Set 2

n			ML	MPS	MSALD	LS	WLS	Pe	AD	LAD	LTS	CM
50	RAbias	$\hat{\varsigma}$	0.1316	0.2265	0.1505	0.1133	0.0904	0.1389	0.0926	0.1055	0.1790	0.1477
		$\hat{\psi}$	0.2671	0.3752	0.4841	0.3421	0.2294	0.2574	0.2226	0.4278	0.5436	0.3602
		$\hat{\nu}$	0.8094	0.9086	0.8393	0.8687	0.6845	0.6659	0.6819	0.9221	0.8110	0.8789
	MSE	$\hat{\varsigma}$	1.6944	2.9454	2.2266	1.7391	1.2347	1.7967	1.0388	1.2802	2.6730	1.9793
		$\hat{\psi}$	0.4053	0.7593	1.3503	0.8023	0.3677	0.6959	0.3175	0.9237	1.9273	0.7683
		$\hat{\nu}$	0.2952	0.3621	0.3400	0.3354	0.2172	0.2637	0.2064	0.3307	0.4181	0.3440
80	RAbias	$\hat{\varsigma}$	0.0525	0.0972	0.0671	0.0485	0.0375	0.0759	0.0418	0.0463	0.0835	0.0676
		$\hat{\psi}$	0.1586	0.1913	0.2425	0.2178	0.1622	0.1159	0.1260	0.2860	0.6446	0.2346
		$\hat{\nu}$	0.4384	0.5114	0.6813	0.6444	0.4350	0.4543	0.4241	0.6862	1.0768	0.6659
	MSE	$\hat{\varsigma}$	0.4903	0.6788	0.8320	0.7367	0.4945	0.8676	0.4541	0.5367	1.1954	0.7942
		$\hat{\psi}$	0.2318	0.2851	0.3900	0.2825	0.2767	0.1923	0.1011	0.4718	1.9513	0.3095
		$\hat{\nu}$	0.0927	0.1297	0.2061	0.1685	0.0853	0.1282	0.0814	0.1921	0.4910	0.1817
150	RAbias	$\hat{\varsigma}$	0.0285	0.0516	0.0304	0.0246	0.0206	0.0446	0.0224	0.0252	0.0291	0.0341
		$\hat{\psi}$	0.0586	0.0735	0.1018	0.1010	0.0624	0.0437	0.0624	0.1142	0.4860	0.1066
		$\hat{\nu}$	0.1933	0.2070	0.3385	0.3318	0.2131	0.2101	0.2095	0.3337	0.9792	0.3355
	MSE	$\hat{\varsigma}$	0.2203	0.2650	0.3613	0.3276	0.2319	0.3943	0.2239	0.2550	0.5030	0.3413
		$\hat{\psi}$	0.0400	0.0460	0.0825	0.0761	0.0420	0.0546	0.0398	0.0878	1.0152	0.0788
		$\hat{\nu}$	0.0293	0.0328	0.0664	0.0558	0.0294	0.0422	0.0289	0.0596	0.3413	0.0572
250	RAbias	$\hat{\varsigma}$	0.0139	0.0282	0.0145	0.0118	0.0089	0.0256	0.0107	0.0109	0.0037	0.0174
		$\hat{\psi}$	0.0367	0.0455	0.0528	0.0603	0.0412	0.0271	0.0402	0.0707	0.3916	0.0630
		$\hat{\nu}$	0.1155	0.1201	0.1766	0.1922	0.1332	0.1255	0.1287	0.2029	0.8083	0.1927
	MSE	$\hat{\varsigma}$	0.1128	0.1279	0.1749	0.1741	0.1225	0.2193	0.1208	0.1345	0.2637	0.1783
		$\hat{\psi}$	0.0204	0.0226	0.0318	0.0369	0.0226	0.0295	0.0216	0.0400	0.7151	0.0375
		$\hat{\nu}$	0.0134	0.0146	0.0228	0.0247	0.0148	0.0203	0.0142	0.0260	0.2473	0.0250
350	RAbias	$\hat{\varsigma}$	0.0092	0.0194	0.0066	0.0045	0.0043	0.0186	0.0054	0.0047	0.0025	0.0085
		$\hat{\psi}$	0.0265	0.0330	0.0440	0.0521	0.0346	0.0203	0.0337	0.0556	0.3391	0.0539
		$\hat{\nu}$	0.0867	0.0893	0.1454	0.1634	0.1118	0.0968	0.1083	0.1600	0.6363	0.1636
	MSE	$\hat{\varsigma}$	0.0783	0.0853	0.1196	0.1217	0.0872	0.1585	0.0848	0.0925	0.1940	0.1235
		$\hat{\psi}$	0.0130	0.0141	0.0212	0.0247	0.0156	0.0201	0.0150	0.0252	0.7010	0.0250
		$\hat{\nu}$	0.0086	0.0092	0.0150	0.0167	0.0104	0.0137	0.0100	0.0162	0.1631	0.0168

Table 6. Parameter estimates of simulation results for Set 3

n			ML	MPS	MSALD	LS	WLS	Pe	AD	LAD	LTS	CM
50	RAbias	$\hat{\varsigma}$	0.1791	0.3015	0.1823	0.1344	0.1129	0.2572	0.1153	0.1193	0.1879	0.1720
		$\hat{\psi}$	0.1437	0.1597	0.2993	0.2257	0.1714	0.3361	0.1590	0.2436	0.4632	0.2470
		$\hat{\nu}$	0.8398	0.8279	1.0045	1.0867	0.9132	1.2787	0.9235	1.0168	1.1483	1.1001
	MSE	$\hat{\varsigma}$	2.0264	3.2419	2.2239	1.6331	1.3098	3.1125	1.1346	1.2163	2.0752	1.8639
		$\hat{\psi}$	0.1009	0.1309	0.2700	0.1567	0.1269	0.3645	0.0869	0.1460	0.5800	0.1739
		$\hat{\nu}$	0.0383	0.0432	0.0505	0.0518	0.0376	0.0714	0.0400	0.0440	0.0684	0.0539
80	RAbias	$\hat{\varsigma}$	0.0806	0.1460	0.0919	0.0640	0.0492	0.1777	0.0515	0.0561	0.0970	0.0841
		$\hat{\psi}$	0.0839	0.0854	0.1687	0.1590	0.1031	0.2071	0.1016	0.1457	0.4578	0.1693
		$\hat{\nu}$	0.5235	0.4940	0.8139	0.8472	0.6231	1.1686	0.5935	0.7512	1.1185	0.8584
	MSE	$\hat{\varsigma}$	0.6630	0.9813	0.9804	0.7954	0.5571	2.0840	0.4958	0.5398	1.0858	0.8536
		$\hat{\psi}$	0.0389	0.0468	0.1180	0.0873	0.0399	0.1692	0.0393	0.0533	0.4849	0.0938
		$\hat{\nu}$	0.0163	0.0182	0.0307	0.0297	0.0181	0.0540	0.0163	0.0252	0.0535	0.0310
150	RAbias	$\hat{\varsigma}$	0.0395	0.0730	0.0422	0.0332	0.0262	0.1153	0.0270	0.0297	0.0375	0.0432
		$\hat{\psi}$	0.0341	0.0305	0.0683	0.0712	0.0476	0.0868	0.0490	0.0694	0.2967	0.0748
		$\hat{\nu}$	0.2356	0.1938	0.4382	0.4388	0.3026	0.7185	0.3011	0.3600	0.9733	0.4383
	MSE	$\hat{\varsigma}$	0.2362	0.3037	0.3877	0.3536	0.2462	1.1463	0.2358	0.2454	0.4712	0.3684
		$\hat{\psi}$	0.0135	0.0147	0.0257	0.0232	0.0149	0.0459	0.0143	0.0209	0.1923	0.0239
		$\hat{\nu}$	0.0054	0.0055	0.0127	0.0102	0.0059	0.0243	0.0059	0.0078	0.0382	0.0103
250	RAbias	$\hat{\varsigma}$	0.0193	0.0402	0.0188	0.0159	0.0113	0.0712	0.0126	0.0129	0.0077	0.0217
		$\hat{\psi}$	0.0235	0.0200	0.0391	0.0452	0.0331	0.0493	0.0328	0.0468	0.2243	0.0470
		$\hat{\nu}$	0.1448	0.1101	0.2438	0.2617	0.1907	0.4189	0.1868	0.2307	0.7961	0.2597
	MSE	$\hat{\varsigma}$	0.1142	0.1350	0.1755	0.1853	0.1262	0.6483	0.1233	0.1254	0.2396	0.1902
		$\hat{\psi}$	0.0074	0.0079	0.0115	0.0124	0.0084	0.0240	0.0081	0.0113	0.1212	0.0125
		$\hat{\nu}$	0.0026	0.0026	0.0047	0.0047	0.0030	0.0105	0.0029	0.0040	0.0281	0.0047
350	RAbias	$\hat{\varsigma}$	0.0123	0.0275	0.0084	0.0055	0.0049	0.0515	0.0058	0.0059	0.0000	0.0095
		$\hat{\psi}$	0.0183	0.0157	0.0351	0.0416	0.0288	0.0385	0.0287	0.0382	0.1993	0.0429
		$\hat{\nu}$	0.1134	0.0858	0.2025	0.2243	0.1592	0.3260	0.1572	0.1840	0.6474	0.2226
	MSE	$\hat{\varsigma}$	0.0797	0.0896	0.1199	0.1247	0.0877	0.4450	0.0856	0.0866	0.1729	0.1267
		$\hat{\psi}$	0.0050	0.0052	0.0078	0.0086	0.0058	0.0170	0.0057	0.0075	0.1369	0.0087
		$\hat{\nu}$	0.0017	0.0017	0.0030	0.0032	0.0021	0.0069	0.0021	0.0026	0.0195	0.0033

7.Real Data Analysis

In this section, two popular data sets are used to exhibit the effectiveness of the presented model. It also includes data analysis to evaluate the UIPL model's goodness-of-fit compared to other competitive models.

Data I

The data include 38 days of Saudi Arabian Covid-19 data, spanning from July 22, 2021, to August 28, 2021, provided by Alotaibi et al. (2024). These results illustrate the drought mortality rate. The following data are:

0.2375, 0.2962, 0.2167, 0.2752, 0.2353, 0.2347, 0.1951, 0.2140, 0.2329, 0.2711, 0.2126, 0.2314, 0.1924, 0.2113, 0.2683, 0.2487, 0.2674, 0.1716, 0.2666, 0.2091, 0.2278, 0.1706, 0.2271, 0.1890, 0.2077, 0.2452, 0.1319, 0.2259, 0.1504, 0.1879, 0.1689, 0.2063, 0.2249, 0.1686, 0.1310, 0.1497, 0.1309, 0.1495.

The data sets that are being proposed have multiple descriptive statistics displayed in Table 7.

Data II

This dataset, household food expenditures, is provided by Zeileis et al. (2016). The data examines how much money 38 families in a major American city spend on food. It specifically looks at the portion of these families' income that goes toward food expenses. The data also includes the number of people residing in each household and the families' perceived income levels. The percentages of income related to food as well as reading accuracy ratings are taken into account. The data is presented as follows

0.2560663, 0.2023231, 0.2911260, 0.1898036, 0.1619337, 0.3682923, 0.2800173, 0.2067752, 0.1604955, 0.2280656, 0.1921144, 0.2541947, 0.3015883, 0.2570303, 0.2914370, 0.3624967, 0.2265521, 0.3086045, 0.3705066, 0.1075258, 0.3306025, 0.2590826, 0.2501853, 0.2387817, 0.4144203, 0.1782736, 0.2250664, 0.2630519, 0.3652334, 0.5612430, 0.2423906, 0.3418765, 0.3485698, 0.3284759, 0.3508731, 0.2353782, 0.5140399, 0.5429749.

Table 7. Descriptive summary datasets

Dataset	Min	Q_1	Median	Mean	Q_3	Max	Variance	Skewness	Kurtosis
I	0.1309	0.1757	0.2133	0.2100	0.2352	0.2962	0.0019	-0.1692	2.2891
II	0.1075	0.2269	0.2611	0.2897	0.3469	0.5612	0.0103	0.9427	3.8595

Figures 7 and 8 display some graphical representations of these two datasets, respectively. These consist of quantile-quantile (QQ) plots, box plots, violin plots, histograms, kernel density estimates, and total time on test plots. The purpose of these plots is to Verify that the data is suitable and reliable for depicting the corresponding data sets.

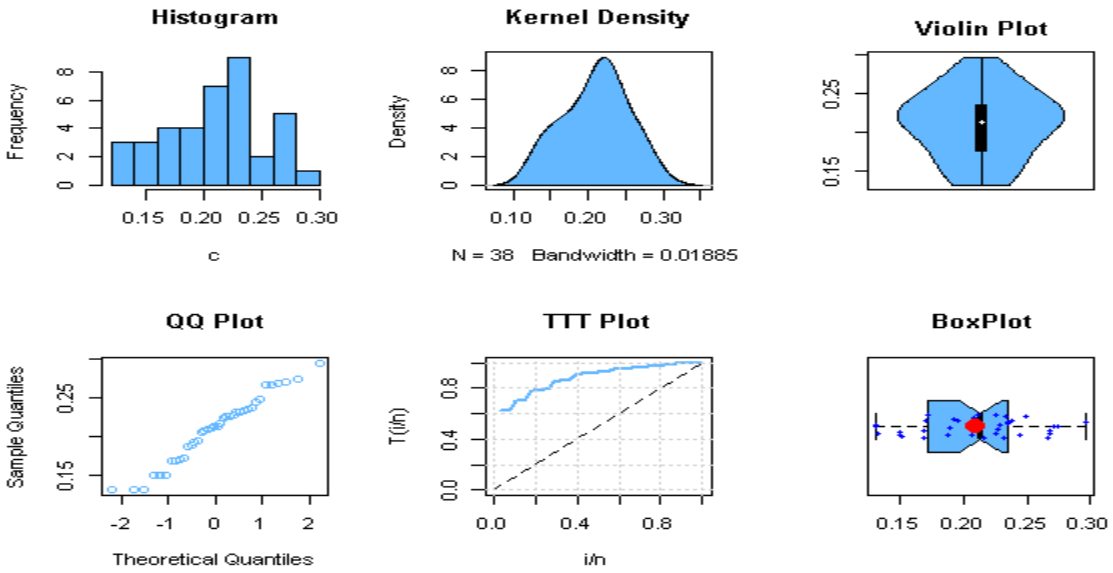

Figure 7. Simple informal graphs for data I.

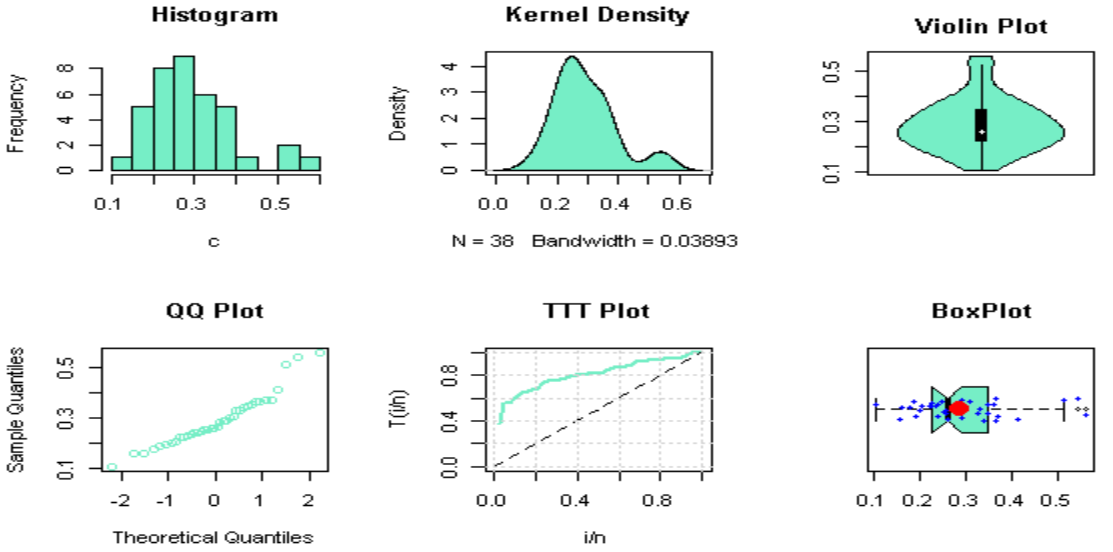

Figure 8. Simple informal graphs for data II.

Data I is mainly left-skewed with some outliers and has an increasing Hrf, as these figures demonstrate, while data II is almost symmetrical and has an increasing Hrf. According to the theoretical results, the UIPL model is capable of handling these characteristics.

Various distributions are recommended for comparison with UIPL including, unit power Lomax (UPL) which was presented by Hassan et al. (2024), unit exponentiated Lomax (UEL) which was proposed by Fayomi et al. (2023), unit Weibull (UW) which was obtained by Mazucheli et al. (2020), unit Gompertz (UG), Kumaraswamy model (KM) which was obtained by Kumaraswamy (1980). Tables 8 and 10, respectively, contain all parameter estimates and standard errors (StErs) for the two real datasets.

Measures of goodness-of-fit for suggested models such as minus two log-likelihood (-2logL), Akaike Information Criterion (Υ_1), Bayesian Information Criterion (Υ_2), Corrected Akaike

Information Criterion(Υ_3), Hannan-Quinn Information Criterion(Υ_4), Kolmogorov-Smirnov (Υ_5) statistic, p-value, Cramer-von Mises (W) test statistic, and Anderson-Darling (A) test statistic are used.

The model with the minimum values for (-2logL), Υ_1, Υ_2, Υ_3, Υ_4, Υ_5, A and W and has maximum p-value can be considered the model that best fits the data among the alternatives presented.

For data I, Table 9 displays the measures of goodness-of-fit for all models. Figure 9 displays plots of estimated CDFs and histograms with the estimated PDFs of all examined models. Figure 10 display, PP plots for UIPL model with comparative distributions.

Table 8. Estimated parameters with the StEr of all the compared models for data I

Model	ψ	ς	υ	$StEr(\psi)$	$StEr(\varsigma)$	$StEr(\upsilon)$
UIPL	4.7841	9.6106	0.0997	8.8495	2.2227	0.2893
UPL	0.8120	11.4367	100.3558	0.4148	2.3454	50.5221
UEL	0.0354	110.9134	292.9375	0.0163	49.8073	132.9154
UW	0.0207	7.4712	—	0.0110	0.8727	—
UG	0.0022	3.6530	—	0.0003	0.1222	—
KM	3.4316	157.5982	—	0.2798	61.9819	—

Table 9. Different measures of goodness-of-fit for data I

Name	**-2logL**	Υ_1	Υ_2	Υ_3	Υ_4	Υ_5	**p-value**	**W**	**A**
UIPL	-131.5631	-125.5631	-120.6504	-124.8572	-123.8152	0.0799	0.9525	0.0351	0.2915
UPL	-127.5035	-121.5035	-116.5908	-120.7977	-119.7556	0.1179	0.6239	0.0549	0.3848
UEL	-123.2296	-117.2296	-112.3168	-116.5237	-115.4817	0.1361	0.4431	0.0461	0.3253
UW	-123.9985	-119.9985	-116.7233	-119.6556	-118.8332	0.1653	0.2240	0.2015	1.2104
UG	-116.9561	-112.9561	-109.6809	-112.6132	-111.7908	0.1903	0.1117	0.2466	1.4743
KM	-119.6590	-115.6590	-112.3838	-115.3161	-114.4937	0.1379	0.4268	0.0503	0.3466

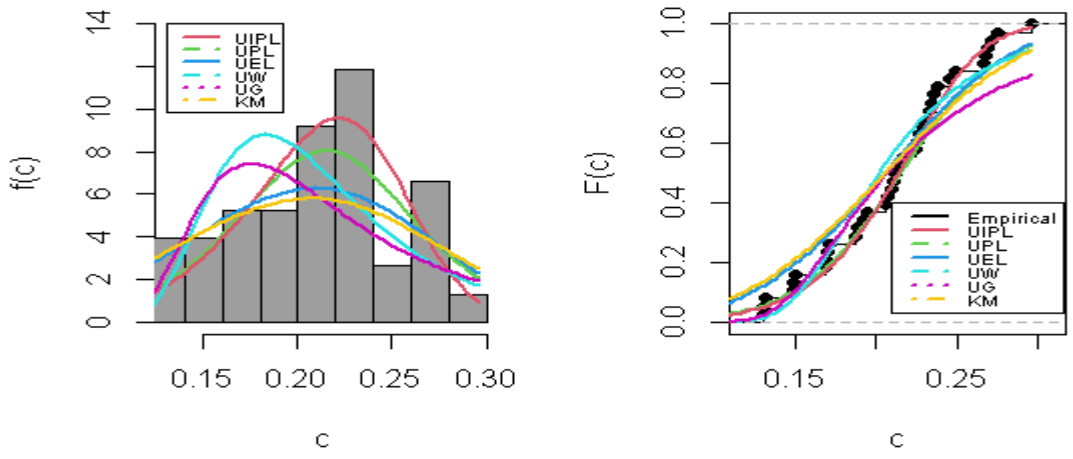

Figure 9. Plots representing the estimated CDFs and PDFs for data I

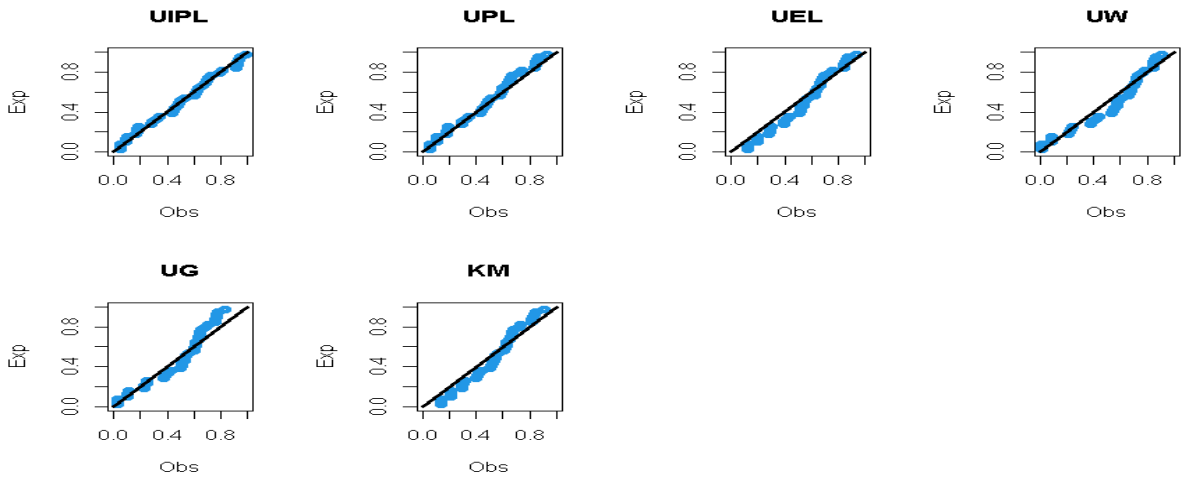

Figure 10. PP plots for UIPL model with comparative distributions for data I

For data II, Table 11 displays measures of goodness-of-fit for compared models. Figure 11 display plots of estimated CDFs and histograms with estimated PDFs of all examined models. Figure 12 display, PP plots for UIPL model with comparative distributions.

Table 10. Estimated parameters with the StErs of all the compared models for data II

Model	ψ	ς	υ	$StEr(\psi)$	$StEr(\varsigma)$	$StEr(\upsilon)$
UIPL	0.4143	9.9934	0.0166	0.1849	2.7822	0.0288
UPL	3.5174	4.9884	16.4179	3.8957	1.0336	18.0358
UEL	0.0415	74.3643	28.7214	0.0414	71.0655	11.9412
UW	0.2320	4.1288	—	0.0656	0.4995	—
UG	0.0211	2.6569	—	0.0121	0.3310	—
KM	2.9546	26.9643	—	0.3692	10.8248	—

Table 11. Different measures of goodness-of-fit for data II

Model	**-2logL**	Υ_1	Υ_2	Υ_3	Υ_4	Υ_5	**p-value**	**W**	**A**
UIPL	-73.3992	-67.3992	-62.4864	-66.6933	-65.6513	0.0715	0.9825	0.0253	0.1855
UPL	-73.0579	-67.0579	-62.1451	-66.3520	-65.3100	0.0800	0.9520	0.0308	0.2351
UEL	-66.5617	-60.5617	-55.6490	-59.8559	-58.8138	0.1257	0.5438	0.1246	0.8984
UW	-71.8687	-67.8687	-64.5936	-67.5259	-66.7034	0.0964	0.8386	0.0389	0.2964
UG	-65.2801	-61.2801	-58.0049	-60.9372	-60.1148	0.1345	0.4579	0.0934	0.6481
KM	-66.9782	-62.9782	-59.7030	-62.6353	-61.8129	0.1237	0.5642	0.1193	0.8627

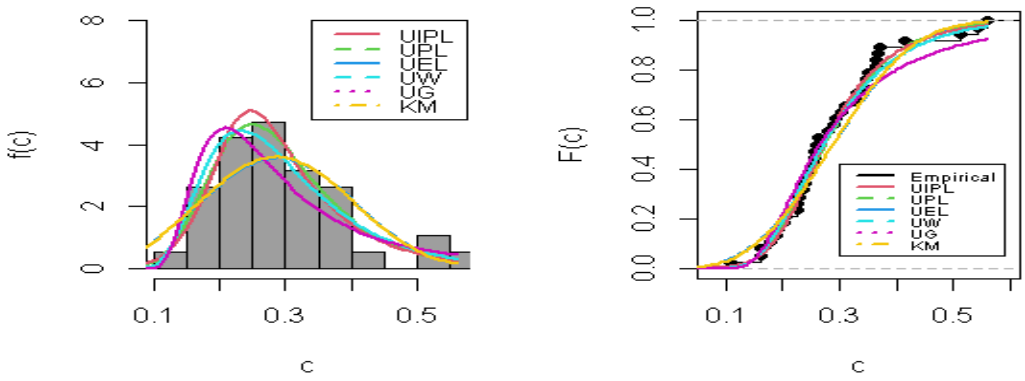

Figure 11. Plots representing the estimated CDFs and PDFs for data II

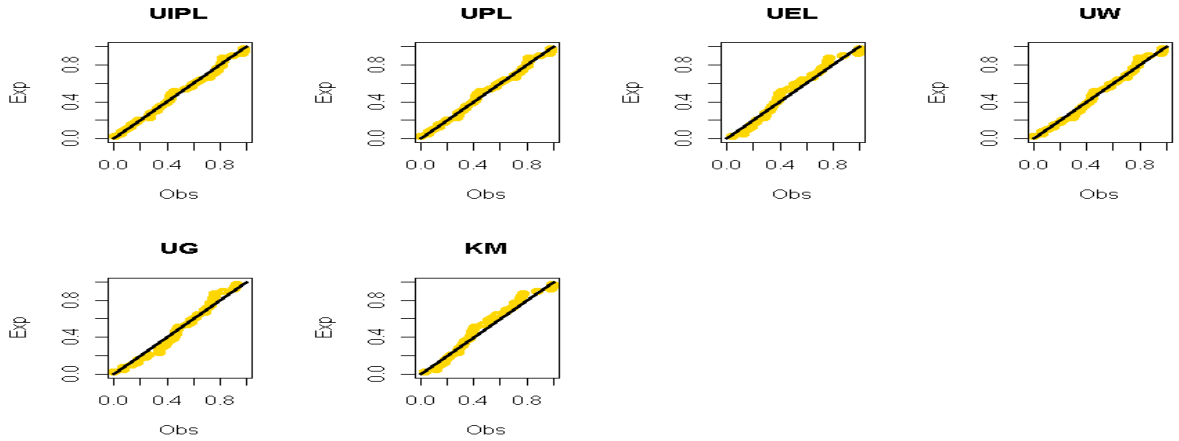

Figure 12. PP plots for UIPL model with comparative distributions for data II

8. Conclusion

In this work, a new bounded distribution was presented as an alternative to multiple new bounded distributions, referred to as the unit inverse power Lomax model. Its PDF can be decreasing, increasing, or right-skewed, according to an analysis. Conversely, the Hrf may exhibit a bathtub-shaped, J-shaped, or an increasing pattern. The quantile, median, skewness, kurtosis, moments, variance, coefficient of variation, incomplete moments, Lorenz curve, probability weighted moment, order statistics, and stress-strength reliability are among the many measures calculated in closed form. The computed uncertainty measures are $R_\delta, E_\delta, T_\delta, A_\delta, HC_\delta, \tau, \tau^w$ and Ω. The estimation techniques of ML, MPS, MSALD, LS, WLS, Pe, AD, LAD, LTS, and CM are employed to estimate the unknown parameters of the proposed UIPL model. The asymptotic behavior of the parameter estimations for the UIPL was investigated using a numerical simulated study, and it was concluded that the AD method was the most effective approach in most circumstances. The importance of the UIPL model in comparison to other well-known statistical models, including the unit power Lomax, unit exponentiated Lomax distribution, unit Weibull, unit Gompertz, and Kumaraswamy distribution, is demonstrated by two applications employing

actual datasets. This conclusion suggests that the UIPL distribution is a flexible model with unique characteristics, which gives the opportunity of further research in future such as stress-strength estimation, entropy estimation, and more research in different fields.

Declaration of Interest: The authors disclosed that they had no conflicts of interest.

Fundings: This research received no specific grant from any funding agency in the public, commercial, or not-for-profit sectors.

References

Abd AL-Fattah, A. M., El-Helbawy, A. A., and Al-Dayian, G. R. (2017). Inverted Kumaraswamy distribution: properties and estimation. *Pakistan Journal of Statistics, 33*(1): 37–61.

Abe, S., and Suzuki, N. (2003). Law for the distance between successive earthquakes. *Journal of Geophysical Research: Solid Earth, 108*(B2). https://doi.org/10.1029/2002JB002220.

Aguilar, G. A., Moala, F. A., and Cordeiro, G. M. (2019). Zero-truncated poisson exponentiated gamma distribution: application and estimation methods. *Journal of Statistical Theory Practice, 13*: 1–20. https://doi.org/10.1007/s42519-019-0059-2.

Al-Omari, A. I., Alanzi, A. R., and Alshqaq, S. S. (2024). The unit two parameters Mirra distribution: reliability analysis, properties, estimation and applications. *Alexandria Engineering Journal, 92*: 238–253. https://doi.org/10.1016/j.aej.2024.02.063.

Ali, S., Dey, S., Tahir, M. H., and Mansoor, M. (2020). Two-parameter logistic-exponential distribution: some new properties and estimation methods. *American Journal of Mathematical Management Sciences, 39*(3): 270–298. https://doi.org/10.1080/01966324.2020.1728453.

Alotaibi, N., Al-Moisheer, A. S., Hassan, A. S., Elbatal, I., Alyami, S. A., and Almetwally, E. M. (2024). Epidemiological modeling of COVID-19 data with Advanced statistical inference based on Type-II progressive censoring. *Heliyon, 10*(18). https://doi.org/10.1016/j.heliyon.2024.e36774.

Arimoto, S. (1971). Information-theoretical considerations on estimation problems. *Information and Control, 19*(3), 181–194. https://doi.org/10.1016/S0019-9958(71)90065-9.

Atkinson, A. B., and Harrison, A. J. (1978). *Distribution of Personal Wealth in Britain*: Cambridge University Press.

Bakouch, H. S., Hussain, T., Tošić, M., Stojanović, V. S., and Qarmalah, N. (2023). Unit exponential probability distribution: Characterization and applications in environmental and engineering data modeling. *Mathematics, 11*(19), 4207. https://doi.org/10.3390/math11194207.

Balakrishnan, N., Buono, F., and Longobardi, M. (2022). On weighted extropies. *Communications in Statistics-Theory Methods, 51*(18): 6250–6267. https://doi.org/10.1080/03610926.2020.1860222.

Beck, C. (2009). Generalised information and entropy measures in physics. *Contemporary Physics, 50*(4): 495-510. http://dx.doi.org/10.1080/00107510902823517.

Birnbaum, Z. W. (1956). *On a Use of the Mann-Whitney Statistic* (Vol. 1). USA: University of California Press Berkeley.

Campbell, L. L. (1966). Exponential entropy as a measure of extent of a distribution. *Zeitschrift für Wahrscheinlichkeitstheorie und verwandte Gebiete, 5*(3): 217–225. https://doi.org/10.1007/BF00533058.

Cheng, R., and Amin, N. (1979). Maximum product-of-spacings estimation with applications to the lognormal distribution. *Mathematical Reports, 791*.

Elgarhy, M., Elbatal, I., Hassan, A. S., Gemeay, A. M., Diab, L. S., and Ghorbal, A. (2023). The inverse power Zeghdoudi distribution with twelve different methods of estimation and

applications to engineering and environmental data. *Physica Scripta, 99*(6). https://doi.org/10.1088/1402-4896/ad46d0.

Fayomi, A., Hassan, A. S., and Almetwally, E. M. (2023). Inference and quantile regression for the unit-exponentiated Lomax distribution. *Plos one, 18*(7), e0288635. https://doi.org/10.1371/journal.pone.0288635.

Ghitany, M. E., Mazucheli, J., Menezes, A. F. B., and Alqallaf, F. (2019). The unit-inverse Gaussian distribution: A new alternative to two-parameter distributions on the unit interval. *Communications in Statistics-Theory and Methods, 48*(14), 3423–3438. https://doi.org/10.1080/03610926.2018.1476717.

Greenwood, J. A., Landwehr, J. M., Matalas, N. C., and Wallis, J. R. (1979). Probability weighted moments: definition and relation to parameters of several distributions expressable in inverse form. *Water Resources Research, 15*(5): 1049–1054. https://doi.org/10.1029/WR015i005p01049.

Haq, M. A. U., Hashmi, S., Aidi, K., Ramos, P. L., and Louzada, F. (2020). Unit modified Burr-III distribution: estimation, characterizations and validation test. *Annals of Data Science*, *99*(1): 1–26. https://doi.org/10.1007/s40745-020-00298-6.

Hassan, A. S., and Nassr, S. G. (2019). Power Lindley-G family of distributions. *Annals of Data Science, 6*, 189–210. https://doi.org/10.1007/s40745-018-0159-y.

Hassan, A. S., and Alharbi, R. S. (2023). Different estimation methods for the unit inverse exponentiated Weibull distribution. *CSAM (Communications for Statistical Applications and Methods), 30*(2): 191–213. http://doi.org/10.29220/CSAM.2023.30.2.191.

Hassan, A. S., Khalil, A. M., and Nagy, H. F. (2024). Data analysis and classical estimation methods of the bounded power Lomax distribution. *Reliability: Theory Applications, 19*(1 (77)): 770–789.

Havrda, J., and Charvát, F. (1967). Quantification method of classification processes. Concept of structural a-entropy. *Kybernetika, 3*(1): 30–35. https://dml.cz/handle/10338.dmlcz/125526.

Holland, O., Golaup, A., and Aghvami, A. H. (2006). Traffic characteristics of aggregated module downloads for mobile terminal reconfiguration. *IEE proceedings-Communications, 153*(5): 683–690. http://doi.org/10.1049/ip-com_20045155.

Husseiny, I. A., Nagy, M., Mansi, A. H., and Alawady, M. A. (2024). Some Tsallis entropy measures in concomitants of generalized order statistics under iterated FGM bivariate distribution. *AIMS Mathematics, 9*(9), 23268-23290. http://doi.org/10.3934/math.20241131.

Jahanshahi, S. M. A., Zarei, H., and Khammar, A. H. (2020). On cumulative residual extropy. *Probability in the Engineering Informational Sciences, 34*(4): 605–625. https://doi.org/10.1017/S0269964819000196.

Jiang, Z. Q., Chen, W., and Zhou, W. X. (2008). Scaling in the distribution of intertrade durations of Chinese stocks. *Physica A: Statistical Mechanics and its Applications, 387*(23): 5818-5825. https://doi.org/10.1016/j.physa.2008.06.039.

Jónás, T., Chesneau, C., Dombi, J., and Bakouch, H. S. (2022). The inverse epsilon distribution as an alternative to inverse exponential distribution with a survival times data example. *Acta Cybernetica, 25*(3): 613–628. https://doi.org/10.14232/actacyb.292077.

Keller, A. Z., Kamath, A. R. R., and Perera, U. D. (1982). Reliability analysis of CNC machine tools. *Reliability Engineering, 3*(6): 449–473. https://doi.org/10.1016/0143-8174(82)90036-1.

Krishna, A., Maya, R., Chesneau, C., and Irshad, M. R. (2022). The unit Teissier distribution and its applications. *Mathematical Computational Applications, 27*(1), 12. https://doi.org/10.3390/mca27010012.

Kumaraswamy, P. (1980). A generalized probability density function for double-bounded random processes. *Journal of Hydrology, 46*(1-2): 79–88. https://doi.org/10.1016/0022-1694(80)90036-0.

Lad, F., Sanfilippo, G., and Agro, G. (2015). Extropy: Complementary dual of entropy. *Statistical Science*, *30*(1): 40–58. https://doi.org/10.1214/14-STS430.

Lee, S., Noh, Y., and Chung, Y. (2017). Inverted exponentiated Weibull distribution with applications to lifetime data *Communications for Statistical Applications and Methods, 24*(3): 227–240. https://doi.org/10.5351/CSAM.2017.24.3.227.

Lomax, K. S. (1954). Business failures: Another example of the analysis of failure data. *Journal of the American Statistical Association, 49*(268): 847–852. https://doi.org/10.1080/01621459.1954.10501239.

Mazucheli, J., Menezes, A. F. B., and Dey, S. (2019). Unit-Gompertz distribution with applications. *Statistica, 79*(1): 25–43. https://doi.org/10.6092/issn.1973-2201/8497.

Mazucheli, J., Korkmaz, M. Ç., Menezes, A. B., and Leiva, V. (2023). The unit generalized half-normal quantile regression model: formulation, estimation, diagnostics, and numerical applications. *Soft Computing, 27*(1): 279–295. https://doi.org/10.1007/s00500-022-07278-3.

Mazucheli, J., Menezes, A. F. B., Fernandes, L. B., De Oliveira, R. P., and Ghitany, M. E. (2020). The unit-Weibull distribution as an alternative to the Kumaraswamy distribution for the modeling of quantiles conditional on covariates. *Journal of Applied Statistics, 47*(6): 954–974. https://doi.org/10.1080/02664763.2019.1657813.

Mohammadi, M., Hashempour, M., and Kamari, O. (2024). On the dynamic residual measure of inaccuracy based on extropy in order statistics. *Probability in the Engineering Informational Sciences, 38*(3):481-502. https://doi.org/10.1017/S0269964823000268.

Mood, A. M., Graybill, F. A., and Boes, D. C. (1950). *Introduction to the Theory of Statistics*: McGraw-Hill.

Nwankwo, K. C., Onyeagu, I. S., Nwankwo, C. H., Osuji, G. A., and Onyekwere, C. K. (2021). On the characteristics and application of inverse power Pranav distribution. *Journal of Advances in Mathematics and Computer Science, 36*(7): 52–65.

Okorie, I. E., Afuecheta, E., and Bakouch, H. S. (2023). Unit upper truncated Weibull distribution with extension to 0 and 1 inflated model–Theory and applications. *Heliyon, 9*(11). https://doi.org/10.1016/j.heliyon.2023.e22260.

Onyekwere, C. K., Osuji, G. A., and Enogwe, S. U. (2020). Inverted power Rama distribution with applications to life time data. *Asian Journal of Probability and Statistics, 9*(4), 1–21.

Opone, F., and Chesneau, C. (2024). Study of the inverse continuous Bernoulli distribution. *Malaya Journal of Matematik, 12*(03): 253–261. https://doi.org/10.26637/mjm1203/003.

Rady, E. H. A., Hassanein, W. A., and Elhaddad, T. A. (2016). The power Lomax distribution with an application to bladder cancer data. *SpringerPlus, 5*: 1–22. https://doi.org/10.1186/s40064-016-3464-y.

Rényi, A. (1961). *On measures of entropy and information.* Paper presented at the Proceedings of the fourth Berkeley symposium on mathematical statistics and probability, volume 1: contributions to the theory of statistics. 4: 547–562.

Shafiq, A., Sindhu, T. N., Hussain, Z., Mazucheli, J., and Alves, B. (2023). A flexible probability model for proportion data: Unit Gumbel type-II distribution, development, properties, different method of estimations and applications. *Austrian Journal of Statistics, 52*(2): 116–140. https://doi.org/10.17713/ajs.v52i2.1407.

Sharma, V. K., Singh, S. K., Singh, U., and Agiwal, V. (2015). The inverse Lindley distribution: a stress-strength reliability model with application to head and neck cancer data. *Journal of*

Industrial Production Engineering, 32(3): 162–173. https://doi.org/10.1080/21681015.2015.1025901.

Soares, A. D., Moura Jr, N. J., and Ribeiro, M. B. (2016). Tsallis statistics in the income distribution of Brazil. *Chaos, Solitons & Fractals, 88*: 158-171. https://doi.org/10.1016/j.chaos.2016.02.026.

Tahir, M. H., Cordeiro, G. M., Ali, S., Dey, S., and Manzoor, A. (2018). The inverted Nadarajah–Haghighi distribution: estimation methods and applications. *Journal of Statistical Computation and Simulation, 88*(14): 2775–2798. https://doi.org/10.1080/00949655.2018.1487441.

Tsallis, C. (1988). Possible generalization of Boltzmann-Gibbs statistics. *Journal of Statistical Physics, 52*: 479–487. https://doi.org/10.1007/BF01016429.

Zeileis, A., Cribari-Neto, F., Gruen, B., Kosmidis, I., Simas, A. B., Rocha, A. V., and Zeileis, M. A. (2016). Package 'betareg'.